Islamic Azad University

Journal of
Optoelectronical Nanostructures

Winter 2024 / Vol. 9, No. 1

## Research Paper

# Electric Field and Impurity Effects on the Electronic Levels and Optical Properties of Spherical Segment Quantum Dot/Wetting Layer Interacted with Two Laser Fields

**Reyhane Ezadi, Masoomeh Dezhkam ***
Department of Physics, Marvdasht Branch, Islamic Azad University, Marvdasht, Iran

**Received: 4 Feb. 2024**
**Revised: 22 Feb. 2024**
**Accepted: 1 Mar. 2024**
**Published: 15 Mar. 2024**

**Use your device to scan and read the article online**

**Keywords:**
**Electric Field, Group Velocity of Light, Impurity, Optical Property, Quantum Dot/Wetting Layer**

## Abstract

We calculate electronic levels of spherical segment quantum dot on top of wetting layer with and without hydrogenic impurity interacted with external electric field numerically. Results show that as the electric field increases, the three lowest level energies decrease. The binding energy of the ground (first excited) state of the system decreases (increases) as the electric field increases. Then we consider the system influenced by two laser fields and investigate the optical properties of the system at the electric field. As results show, the linear and nonlinear absorptions and dispersions of the probe pulse shift to higher frequencies as the electric field increases. For the certain electric field, the optical properties reduce and shift toward higher frequencies when impurity is added. Finally, the group velocity of the probe pulse in the system is calculated. As the electric field increases, the slow light frequency range transfers to the higher probe frequencies.

Citation: Reyhane Ezadi, Masoomeh Dezhkam. Electric Field and Impurity Effects on the Electronic Levels and Optical Properties of Spherical Segment Quantum Dot/Wetting Layer Interacted with Two Laser Fields. **Journal of Optoelectronical Nanostructures. 2024; 9 (1): 79- 95. DOI: 10.30495/JOPN.2024.32976.1311**

***Corresponding author:** Masoomeh Dezhkam
**Address:** Department of Physics, Marvdasht Branch, Islamic Azad University, Marvdasht, Iran. **Tell:** 009891300012 **Email:** dezh@miau.ac.ir

## 1. INTRODUCTION

Quantum dots (QDs), with three-dimensional confinement of carriers, are one of interesting scientific topics. Some of important applications of QDs are: quantum dot lasers [1-2], quantum dot solar cells [3-4], quantum dot photodetectors [5-6] and biomedical applications [7]. Electronic levels and optical properties of QDs have been investigated for different geometries [8-12]. Leonard et al have observed QDs with shape of spherical segment QD (SSQD) in their experiments [13]. Properties of SSQD with wetting layer (WL) were studied [14]. Electronic structure and optical properties of two vertically coupled SSQDs/WLs were investiated [15]. Furthermore, effects of temperature and hydrostatic pressure on the properties of SSQDs/WL were studied [16]. Electric field is one of parameters that affect the electronic and optical properties of QD systems. Some papers are: the effects of electric field on properties of spherical QD at the center of a nanowire [17], the electric field effect on impurity binding energy in wedge-shaped cylindrical QDs [18], effect of an electric field on recombination radiation in QDs [19], effect of electric field on nonlinear optical properties of QDs with multitype-tunable shape [20], the optical properties of the Mathieu QD with the external electric, magnetic and laser field [21]. In this paper, we consider a SSQDs/WL with and without impurity, apply an external electric field and calculate the electronic structure (2A) and optical parameters (2B) of the system interacted with two fields. Furthermore, group velocity of light in QD systems has studied [22-23], so we calculate the group velocity of probe pulse (GVPP) in SSQD/WL with and without impurity (2C).

## 2. INFLUENCE OF ELECTRIC FIELD ON SSQD/WL

### *A. Electronic levels*

We consider an InAs SSQD with a WL in a GaAs barrier. Corresponding to reference [13], we use R =10 nm and h =5 nm. Figure 1 shows the SSQD with WL.

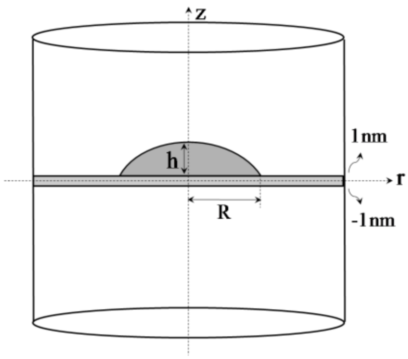


**Fig. 1**. schematic view of SSQD/WL in a GaAs barrier.

We want to investigate electric field effect on the electronic structure of SSQD/WL, without and with (at the origin of the cylindrical coordinates) hydrogenic donor impurity. An external electric field was applied to the system ($\vec{E}_{ext} = E_{ext}\,\hat{k}$). For an electron confined to the system shown in figure 1, the Schrödinger equation in the effective mass approximation can be written as:

$$-\hbar^2/2\vec{\nabla}.(1/m_{eff}(\vec{r})\,\vec{\nabla}u(\vec{r})) + V_{conf}(\vec{r})\,u(\vec{r}) + [V_{e,imp}(\vec{r})u(\vec{r})] - eE_{ext}zu(\vec{r}) = Eu(\vec{r}), \quad (1)$$

where $\hbar$, $m_{eff}(\vec{r})$, $V_{conf}(\vec{r})$, $E$ and $u(\vec{r})$ show Planck's constant divided by $2\pi$, the electron effective mass, the confining potential, the energy and eigenfunction of the electron levels. The term $V_{e,imp}(\vec{r})u(\vec{r})$ is hold only when we add impurity. $V_{e,imp}(\vec{r}) = -e^2/4\pi\varepsilon_0\varepsilon|\vec{r}|$ is the Coulomb interaction between $e$ and impurity, where $e$ is the electronic charge, $\varepsilon_0$ is the permittivity of free space and $\varepsilon$ is the relative dielectric constant. The parameters used to solve the equation (1) were: $m_{eff,InAs} = 0.023m_0$ , $m_{eff,GaAs} = 0.067m_0$ , $V_{conf,InAs} = 0$ and $V_{conf,GaAs} = 0.697eV$ [24-25], $m_0$ is the electron mass. We used $\varepsilon_{InAs} = 14.55$ and $\varepsilon_{GaAs} = 13.18$ [26]. Finite element method has been used to solve the equation (1) numerically (The azimuthal symmetry is seen in this system, so the eigenfunction can be written as $u(r,\phi,z) = A\,g(r,z)\,e^{il\phi}$ : $|l| = 0,1,2,...$ and $A$ is the normalization constant). The boundary conditions were the same as conditions in reference [14]. The energy eigenvalues and eigenfunctions of the system levels have been calculated.

The ground (level 1: L1), first excited state (level 2: L2) and second excited state (level 3: L3) energies as a function of the applied electric field $E_{ext}$ are shown in figure 2. As seen, energies of L1, L2 and L3 decrease as the electric field increases because the term related to the interaction of electron and electric field ($-eE_{ext}zu(\vec{r})$) in the Schrödinger equation (Eq. 1) is negative. The larger the electric field, the lower the level energy. Our results are in good agreement with Turki-Ben Ali et al's. work [25]. It is clear that the energies of the three lowest levels decrease by adding the hydrogenic impurity. Because the Coulomb interaction ($V_{e,imp}(\vec{r}) = -e^2 / 4\pi\varepsilon_0\varepsilon|\vec{r}|$) is negative. This negative term in the Schrödinger equation (Eq. 1) results in a decrease of energies of the three lowest levels.

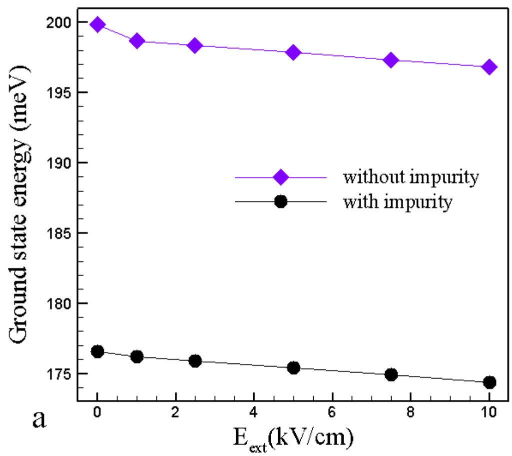

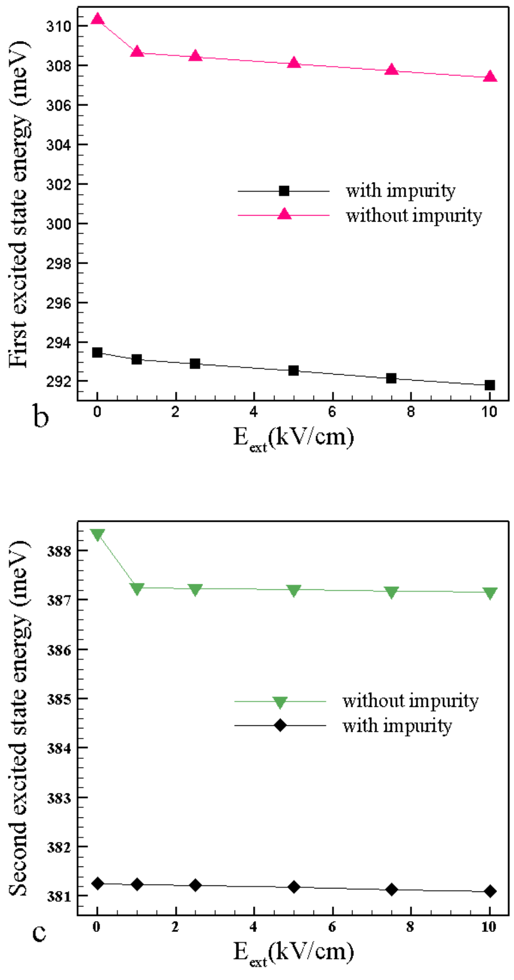


**Fig. 2**. Energies of L1 (a), L2 (b) and L3 (c) for the system with and without impurity as a function of the applied electric field $E_{ext}$ .

Figure 3 shows the binding energy (difference between energies with and without the impurity) of the ground and the first excited states for different values of electric field. The binding energy of the ground state decreases as the electric field increases (figure 3a). The binding energy of L2 increases as the electric field increases (figure 3b).

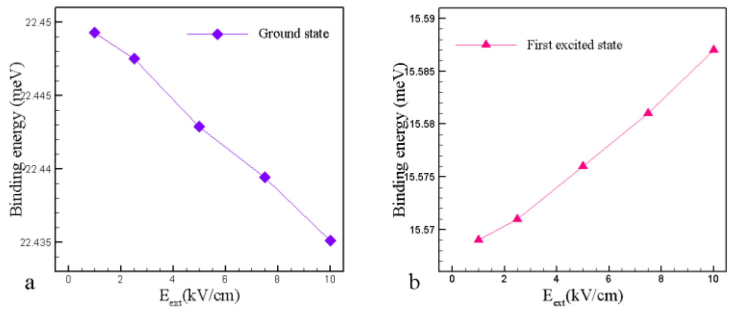


**Fig. 3**. Binding energy as a function of electric field for SSQD/WL.

## *B. Optical properties*

To investigate the optical properties, the system is interacted by an electromagnetic field with *x*-polarization. The dipole moment matrix elements $\mu_{ij} = \left|\langle u_i | e\hat{x} | u_j \rangle\right|$ have been obtained for transitions between two conduction subbands numerically. $u_i$ is the eigenfunction of the *i*th subband. According to $u(r,\phi,z) = A\,g(r,z)\,e^{il\phi}$, only transitions between levels with *l*=0 and *l*=1 are the electric dipole-allowed transitions. For the lowest levels, transitions between 1 and 2 levels and between 2 and 3 levels are the electric dipole-allowed. Transition between 1 and 3 levels is electric dipole-forbidden (figure 4). Therefore, the three levels present a cascade type system.

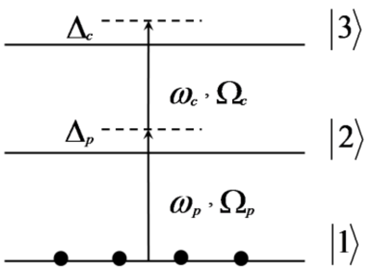


**Fig. 4**. The cascade configuration of SSQD/WL.

SSQD/WL interacts with two laser fields that propagate along *z*- direction. The polarizations of fields are along *x*- direction.

$$\vec{E} = \hat{x} E_p \, e^{(-i\omega_p t + i\vec{k}_p.\vec{r})} + \hat{x} E_c \, e^{(-i\omega_c t + i\vec{k}_c.\vec{r})} + c.c., \quad (2)$$

$E_p$ and $E_c$ are the slowly varying envelopes and $\vec{k}_p$ and $\vec{k}_c$ are the wave vectors of the fields. The weak pulsed probe (strong cw control) field induces transition $|1\rangle \leftrightarrow |2\rangle$ ($|2\rangle \leftrightarrow |3\rangle$) (Figure 4).

As mentioned in references [27-28], the Hamiltonian of SSQD/WL in the interaction picture is:

$$H = -\Delta_p |2\rangle\langle 2| - (\Delta_p + \Delta_c)|3\rangle\langle 3| - (\Omega_c |3\rangle\langle 2| + \Omega_p |2\rangle\langle 1| + H.c.), \quad (3)$$

$\Delta_p = \omega_p - \omega_{21}$ is detuning of the probe field and $\Delta_c = \omega_c - \omega_{32}$ is detuning of the control field. $2\Omega_p = \dfrac{\mu_{21} E_p}{\hbar}$ and $2\Omega_c = \dfrac{\mu_{32} E_c}{\hbar}$ are the Rabi frequencies [27-28], $\mu_{21}$ and $\mu_{32}$ are the dipole moment elements. By using time-dependent Schrödinger equation, linear absorption (LA) and linear dispersion (LD) of the probe pulse can be written as [14]:

$$\mathrm{Im}(\chi^{(1)}(\omega_p)) = \frac{N|\mu_{12}|^2}{2\varepsilon_0 \hbar} \frac{\gamma_2(\Delta_p + \Delta_c)^2 + \gamma_2\gamma_3^2 + \gamma_3 |\Omega_c|^2}{|B|^2}, \quad (4)$$

$$\mathrm{Re}(\chi^{(1)}(\omega_p)) = \frac{N|\mu_{12}|^2}{2\varepsilon_0\hbar}\frac{|\Omega_c|^2(\Delta_p+\Delta_c)-\Delta_p(\Delta_p+\Delta_c)^2-\Delta_p\gamma_3^2}{|B|^2}, \quad (5)$$

the third-order nonlinear absorption (TNA) and third-order nonlinear dispersion (TND) can be written as:

$$\mathrm{Im}(\chi^{(3)}(\omega_p)) = -\frac{N|\mu_{12}|^4}{24\varepsilon_0\hbar^3}\frac{[|\Omega_c|^2+(\Delta_p+\Delta_c)^2+\gamma_3^2][\gamma_2(\Delta_p+\Delta_c)^2+\gamma_2\gamma_3^2+\gamma_3|\Omega_c|^2]}{|B|^4}, \quad (6)$$

$$\mathrm{Re}(\chi^{(3)}(\omega_p)) = -\frac{N|\mu_{12}|^4}{24\varepsilon_0\hbar^3}\times \frac{[|\Omega_c|^2+(\Delta_p+\Delta_c)^2+\gamma_3^2][(\Delta_p+\Delta_c)|\Omega_c|^2-\Delta_p(\Delta_p+\Delta_c)^2-\Delta_p\gamma_3^2]}{|B|^4}. \quad (7)$$

$B = |\Omega_c|^2 - (i\gamma_3+\Delta_p+\Delta_c)\times(i\gamma_2+\Delta_p)$, $\gamma_i$ is the decay rate of level $|i\rangle$, $N$ presents the electron density.

Next, the optical properties of the SSQD/WL system at the electric field $\vec{E}_{ext}$ have been investigated. Figure 5 shows the LA, LD, TNA and TND of the probe pulse via $\omega_p$ for different values of $E_{ext}$ (for the system without impurity). $N = 3\times10^{22} m^{-3}$ [29], $\Omega_c = 9\times10^{12} s^{-1}$, $\gamma_2 = \gamma_3 = 10^{12} s^{-1}$ and $\Delta_c = 2\gamma_2$ were used in calculations.

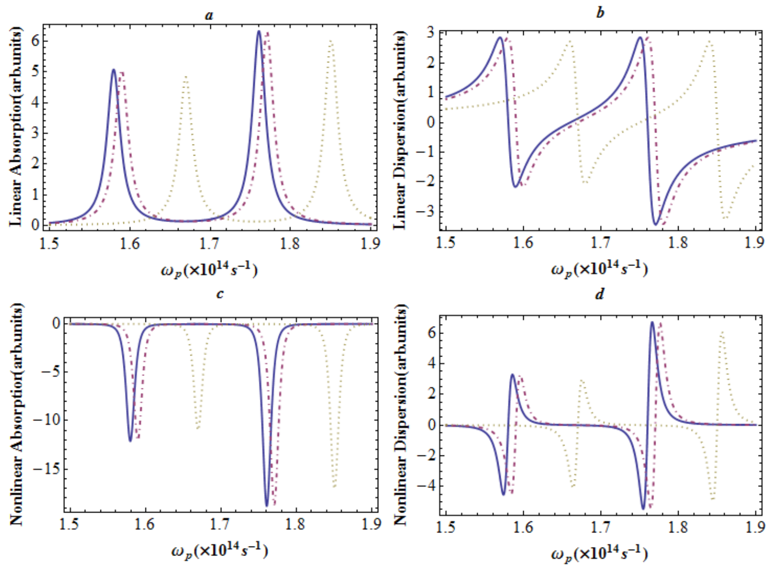


**Fig. 5**. a) LA, b) LD, c) the TNA and d) the TND of the probe pulse as a function of $\omega_p$ for the system without impurity: $E_{ext} = 10^3 V/m$ (the solid line), $E_{ext} = 10^6 V/m$ (dot-dashed line) and $E_{ext} = 10^7 V/m$ (dotted line).

Figure 5 shows that as the electric field increases, the LA, LD, TNA and TND shift toward higher frequencies because the transition energy ($|1\rangle \leftrightarrow |2\rangle$) increases. When the electric field is applied, the energy shifts of levels 1 and 2 are different. This difference increases for larger electric fields. This result is in line with reference [17].

Figure 6 shows the LA, LD, TNA and TND of the probe pulse via $\omega_p$ for different values of $E_{ext}$ (for the system with impurity).

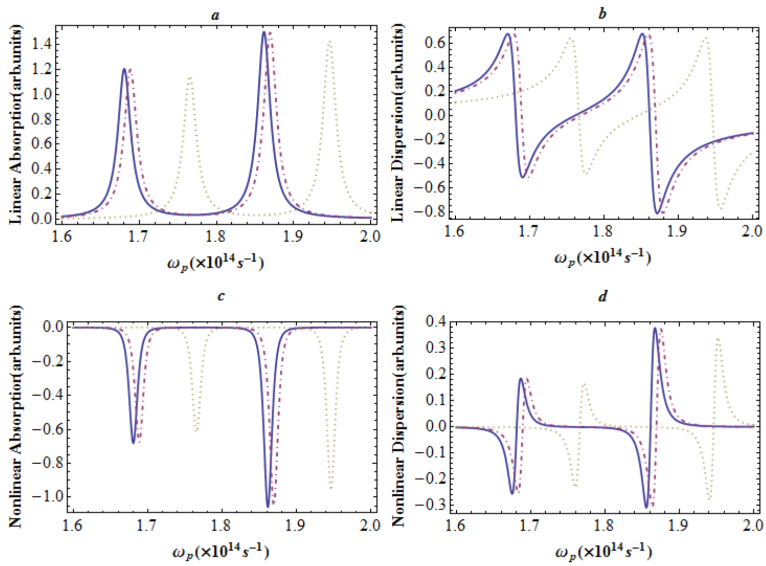


**Fig. 6**. a) LA, b) LD, c) the TNA and d) the TND of the probe pulse via $\omega_p$ for the system with impurity: $E_{ext} = 10^3 V/m$ (the solid line), $E_{ext} = 10^6 V/m$ (dot-dashed line) and $E_{ext} = 10^7 V/m$ (dotted line).

Figure 6 shows that as the electric field increases, the LA, LD, TNA and TND shift toward higher frequencies because the transition energy ($|1\rangle \leftrightarrow |2\rangle$) increases (similar to the system without impurity). The same results had obtained in reference [17].

Figure 7 shows the LA, LD, TNA and TND of the probe pulse via $\omega_p$ for the system with and without impurity ($E_{ext} = 10^6 V/m$).

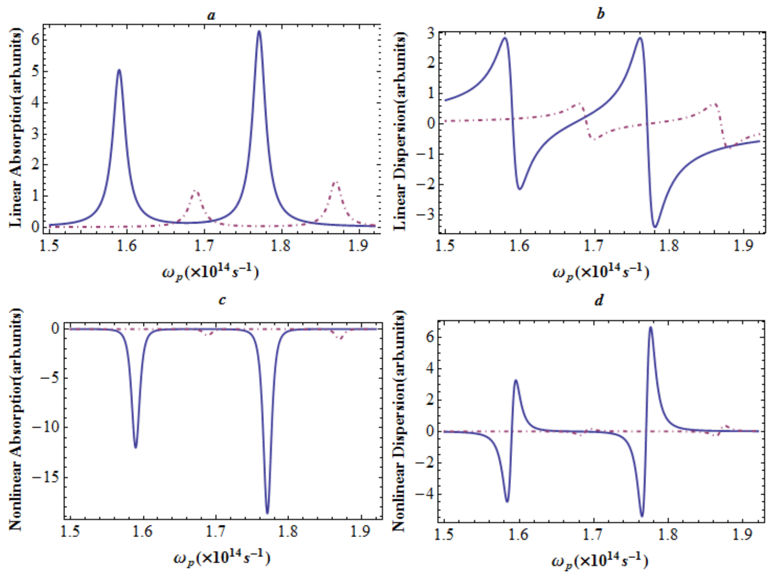


**Fig. 7**. a) LA, b) LD, c) the TNA and d) the TND of the probe pulse via $\omega_p$ for the system without impurity (the solid line) and with impurity (dot-dashed line), $E_{ext} = 10^6 V/m$.

Figure 7 shows that for the certain electric field, the LA, LD, TNA and TND shift toward higher frequencies by inserting hydrogenic impurity. Furthermore, the LA, LD, TNA and TND reduce. This reduction is due to a decrease in the matrix element of the dipole moment $\mu_{21}$ in equations (4)-(7). When the hydrogenic impurity is located at the system, the Coulomb interaction between electron and hydrogenic impurity arises. Consequently, the localization of the electron increases and $\mu_{21} = \left|\langle u_2 | e\hat{x} | u_1 \rangle\right|$ becomes smaller.

## *C. Group velocity of light*

As we know, when two laser fields apply to the system, electromagnetically induced transparency occurs and the GVPP decreases (slow light) [22,30]. The GVPP in the system is [30]:

$$V_g(\omega_p) = \frac{c}{n(\omega_p) + \omega_p \dfrac{dn(\omega_p)}{d\omega_p}}, \tag{8}$$

*n* is the linear refractive index of the system.

Finally, the GVPP in SSQD/WL has been investigated. The GVPP in the system with and without impurity as a function of the probe frequency $\omega_p$ for different electric fields $E_{ext}=10^3, 10^6, 10^7 V/m$ is plotted in Figure 8. The used parameters are: $\gamma_2=\gamma_3=10^{11}s^{-1}$[31], $\Omega_c=1.5\times10^{13}s^{-1}$ and $\Delta_c=0$. As the electric field increases, the slow light frequency range transfers to the higher probe frequencies because the transition frequency increases.

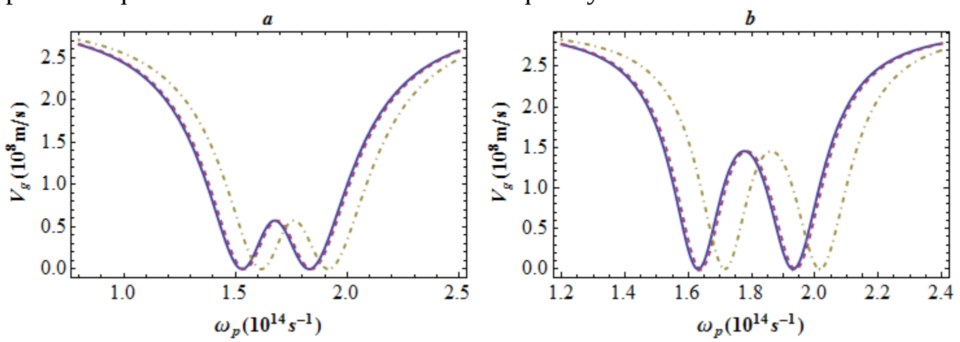


**Fig. 8**. GVPP in the system without (a) and with (b) impurity via the probe frequency $\omega_p$ for different electric fields $E_{ext}=10^3 V/m$ (Solid line), $E_{ext}=10^6 V/m$ (dashed line), $E_{ext}=10^7 V/m$ (dot-dashed line).

## 3. CONCLUSION

In summary, an InAs SSQD/WL in GaAs barrier with and without hydrogenic impurity has been considered. An external electric field has been applied to the quantum dot system. First, the electronic levels of the system have been calculated numerically. Results show that as the electric field increases, the energies of L1, L2, L3 decrease because the term shown the interaction of electron and electric field is negative. L1, L2, L3 energies of the system interacted with electric field decrease when the hydrogenic impurity is added. The binding energy of L1 of the system decreases as the electric field increases but, the binding energy of L2 increases as the electric field increases. Then the system has been considered to interact with two laser fields and the optical properties of the system have been investigated at the electric field. Results show that the LA, LD, TNA and TND for the probe pulse shift toward higher frequencies as the electric field increases because the transition energy increases. The similar results obtain for the system with impurity. For the certain electric field, the LA, LD, TNA and TND of the probe pulse transfer toward higher frequencies when hydrogenic impurity is added. Furthermore, the LA, LD, TNA and TND of the probe pulse reduce. Finally, the GVPP in the system has been calculated for both systems with and without impurity. As the electric field increases, the slow light frequency range shows blue shift because the transition frequency increases.

## REFERENCES

[1] W. Wang, J. Wang, Zh. Cheng, Z. Yang, H. Yin, X. Ma, Y. Zhang, M. Yang, H. Hu, Y. Huang, X. *Numerical Analysis of the Electrically Pumped 1.3 μm InAs/InGaAs Quantum Dot Microdisk Lasers on Silicon with an Output Waveguide*. Ren, Physica E [Online]. 108 (2019, Apr.) 404-410. Available: https://www.sciencedirect.com/science/article/abs/pii/S1386947718308361

[2] N. N. Ledentsov, V. A. Shchukin, Yu. M. Shernyakov, M. M. Kulagina, A. S. Payusov, N. Yu. Gordeev, M. V. Maximov, A. E. Zhukov, L. Ya. Karachinsky, T. Denneulin, N. Cherkashin. *Room Temperature Yellow InGaAlP Quantum Dot Laser*. Solid State Electron. [Online]. 155 (2019, May) 129-138. Available: https://www.sciencedirect.com/science/article/abs/pii/S0038110118305549

[3] A. A. Rajhi, K. M. Abd Alaziz et al. *Enhancing the performance of quantum dot solar cells through halogen adatoms on carboxyl edge-functionalized graphene quantum dots*. Journal of Photochemistry and Photobiology A [Online]. 447 (2024, Jan.) 115240. Available: https://www.sciencedirect.com/science/article/abs/pii/S1010603023007050

[4] D. H. Phuc, H. T. Tung. *Quantum dot sensitized solar cell based on the different photoelectrodes for the enhanced performance*. Sol. Energ. Mat. Sol. C. [Online]. 196 (2019, Jul.) 78–83. Available: https://www.sciencedirect.com/science/article/abs/pii/S0927024819301576

[5] S. Siontas, D. Li, H. Wang, A. A.V.P.S, A. Zaslavsky, D. Pacifici. *High-performance germanium quantum dot photodetectors in the visible and near infrared*. Mat. Sci. Semicon. Proc. [Online]. 92 (2019, Mar.) 19–27. Available: https://www.sciencedirect.com/science/article/abs/pii/S1369800118301896

[6] I. S. Han, J. S. Kim, J. Ch. Shin, J. O. Kim, S. K. Noh, S. J. Lee, S. Krishna. *Photoluminescence study of InAs/InGaAs sub-monolayer quantum dot*

*infrared photodetectors with various numbers of multiple stack layers*. J. Lumin. [Online]. 207 (2019, Mar.) 512-519. Available: https://www.sciencedirect.com/science/article/abs/pii/S0022231318313048

[7] V. G. Reshma, P. V. Mohanan. *Quantum dots: Applications and safety consequences*. J. Lumin. [Online]. 205 (2019, Jan.) 287-298. Available: https://www.sciencedirect.com/science/article/abs/pii/S0022231318313334

[8] M. Servatkhah, P. Hashemi, R. Pourmand. *Binding energy in tuned quantum dots under an external magnetic field*. J. of Optoelectronical Nano Structures. [Online]. 7(4) (2022, Nov.) 49-65. Available: https://jopn.marvdasht.iau.ir/article_5677.html

[9] F. Rahimi, T. Ghaffary, Y. Naimi, H. Khajehazad. *Study the energy states and absorption coefficients of quantum dots and quantum anti-dots with hydrogenic impurity under the applied magnetic field*. J. of Optoelectronical Nano Structures. [Online]. 7(1) (2022, Jan.) 1-18. Available: https://jopn.marvdasht.iau.ir/article_5091.html

[10] A. Jahanshir. *Quanto-Relativistic Background of Strong Electron-Electron Interactions in Quantum Dots under magnetic field*. J. of Optoelectronical Nano Structures. [Online]. 6(3) (2021, Aug.) 1-24. Available: https://jopn.marvdasht.iau.ir/article_4972.html

[11] M. ZekavatFetrat, M. Sabaeian, Gh. Solookinejad. *The effect of ambient temperature on the linear and nonlinear optical properties of truncated pyramidal-shaped InAs/GaAs quantum dot*. J. of Optoelectronical Nano Structures. [Online]. 6(3) (2021, Aug.) 81-92. Available: https://jopn.marvdasht.iau.ir/article_4980.html

[12] H. Bahramiyan, S. Bagheri. *Linear and nonlinear optical properties of a modified Gaussian quantum dot: pressure, temperature and impurity effect*. J. of Optoelectronical Nano Structures. [Online]. 3(3) (2018, Sep.) 79-100. Available:

https://jopn.marvdasht.iau.ir/article_3047.html

[13] D. Leonard, K. Pond, P. M. Petroff. *Critical layer thickness for self-assembled InAs islands on GaAs*. Phys. Rev. B [Online]. 50 (1994, Oct.) 11687–11692. Available: https://journals.aps.org/prb/abstract/10.1103/PhysRevB.50.11687

[14] M. Dezhkam, A. Zakery. *Electronic properties of hemispherical quantum dot/wetting layer with and without hydrogenic donor impurity*. Phys. B [Online]. 443 (2014, Jun.) 70-75. Available: https://www.sciencedirect.com/science/article/abs/pii/S0921452614001859

[15] M. Dezhkam, A. Zakery, A. Keshavarz, Chin. Opt. Lett. 14 (2016) 121904.

[16] Z. Ghafarizadeh Jahromi, M Dezhkam. *Temperature and hydrostatic pressure effects on the electronic structure, optical properties of spherical segment quantum dot/wetting layer and group velocity of light*. Laser Phys. [online]. 30 (2020) 055402. Available: https://doi.org/10.1088/1555-6611/ab8299

[17] M. Moradi, M. Moradi. *The effects of temperature and electric field on the electronic and optical properties of an InAs quantum dot placed at the center of a GaAs nanowire*. J. of surface investigation [online]. 16 (2022) 1237-1247. Available: https://link.springer.com/article/10.1134/S1027451022060428

[18] L. Belamkadem, O. Mommadi et al. *The intensity and direction of the electric field effects on off-center shallow-donor impurity binding energy in wedge-shaped cylindrical quantum dots*. Thin Solid Films [online]. 757 (2022, Sep.) 139396. Available: https://www.sciencedirect.com/science/article/abs/pii/S0040609022003108

[19] V. D. Krevchik, A. V. Razumov et al. *Influence of an external electric field and dissipative tunneling on recombination radiation in quantum dots*. Sensors [online]. 22(4) (2022) 1300. : https://doi.org/10.3390/s22041300 , https://www.mdpi.com/1424-8220/22/4/1300

[20] K. Li, L. Wei, Y. Hu, H. Yin, Z. Li, Z. Chen. *Electric field effect on anisotropic nonlinear optical properties of GaN/AlN quantum dots with multitype-tunable shape*. Optics & Laser Technology [online]. 158 (2023, Feb.) 108797. Available: https://www.sciencedirect.com/science/article/abs/pii/S0030399222009434

[21] M. K. Bahar, P. Baser. *The second, third harmonic generations and nonlinear optical rectification of the Mathieu quantum dot with the external electric, magnetic and laser field***.** Phys. B [online]. 665 (2023, Sep.) 415042.

Available: https://www.sciencedirect.com/science/article/abs/pii/S092145262300409X

[22] V. Pavlović, L. Stevanović. *Group velocity of light in a three level ladder-type spherical quantum dot with hidrogenic impurity*. Superlattice. Microst. [Online]. 100 (2016, Dec.) 500-507. Available: https://www.sciencedirect.com/science/article/abs/pii/S0749603616308448

[23] B. Behroozian, H. R. Askari, M. R. Rezaie. *Light group velocity in quantum dots under electromagnetically induced transparency by using second quantization formalism*. Optik [online]. 226 (2021, Jan.) 165907. Available: https://www.sciencedirect.com/science/article/abs/pii/S0030402620317241

[24] S. S. Li, J. B. Xia, Z. L. Yuan, Z. Y. Xu. *Effective-mass theory for InAs/GaAs strained coupled quantum dots*. Phys. Rev. B [Online]. 54 (1996, Oct.) 11575–11581. Available: https://journals.aps.org/prb/abstract/10.1103/PhysRevB.54.11575

[25] Y. T. B. Ali, G. Bastard, R. Bennaceur. *Ground state transition energies in biased InAs/GaAs quantum dots*. Phys. E [Online]. 27 (2005) 67–76. Available: https://www.sciencedirect.com/science/article/abs/pii/S1386947704005314

[26] E. H. Li. *Material parameters of InGaAsP and InAlGaAs systems for use in quantum well structures at low and room temperatures*. Phys. E [Online]. 5 (2000) 215-273. Available: https://www.sciencedirect.com/science/article/abs/pii/S1386947799002623

[27] W. X. Yang, R. K. Lee. *Slow optical solitons via intersubband transitions in a semiconductor quantum well*. Eur. Phys. Lett. [Online]. 83 (2008, Jul.) 14002. Available: https://iopscience.iop.org/article/10.1209/0295-5075/83/14002/pdf

[28] W. Yan, T. Wang, X. M. Li. *Theoretical ultraslow bright and dark optical solitons in cascade-type GaAs/AlGaAs multiple quantum wells*. Opt. Commun. [Online]. 285 (2012) 3559–3562. Available: https://www.sciencedirect.com/science/article/abs/pii/S0030401812003689

[29] S. Ünlü, İ. Karabulut, H. Şafak. *Linear and nonlinear intersubband optical absorption coefficients and refractive index changes in a quantum box with finite confining potential*. Phys. E [Online]. 33(2) (2006, Jul.) 319-324. Available: https://www.sciencedirect.com/science/article/abs/pii/S1386947706002669

[30] P. W. Milonni, *slow light*, in Fast Light, Slow Light and Left-Handed Light, IOP Publishing, Bristol and Philadelphia, 2005, 144-172.

[31] M. Bayer, A. Forchel. *Temperature dependence of the exciton homogeneous linewidth in In0.60Ga0.40As/GaAs self-assembled quantum dots*. Phys. Rev. B [Online]. 65(4) (2002, Jan.) 041308(R). Available: https://journals.aps.org/prb/abstract/10.1103/PhysRevB.65.041308